JOURNAL OF PROPULSION AND POWER
Vol. 15, No. 6, November–December 1999

Pyrolysis Behavior of Hybrid-Rocket Solid Fuels Under Rapid Heating Conditions

Martin J. Chiaverini,* George C. Harting,† Yeu-Cherng Lu,‡ Kenneth K. Kuo,§ and Arie Peretz¶
Pennsylvania State University, University Park, Pennsylvania 16802
and
H. Stephen Jones,** Brian S. Wygle,** and Joseph P. Arves††
Lockheed Martin Manned Space Systems, New Orleans, Louisiana 70189

An experimental investigation of the thermal pyrolysis behavior of several hybrid-rocket solid fuels under rapid heating conditions was conducted to determine pyrolysis laws and to identify and quantify the products of fuel pyrolysis. The study focused on four fuel formulations: pure hydroxyl-terminated polybutadienes (HTPB), 80% HTPB/20% Alex, 80% HTPB/20% Al, and the Joint Industrial Research and Development fuel formulation. A rapid conductive-heating technique was developed and employed to determine Arrhenius-type pyrolysis laws. All four fuels displayed two sets of Arrhenius parameters, depending on the range of surface temperature. For pure HTPB, E_a = 4.91 kcal/mol and A = 11.04 mm/s above 722 K, while E_a = 13.35 kcal/mol and A = 3965 mm/s below 722 K. These results agree well with those obtained previously using a lab-scale hybrid motor operating under realistic conditions. The gas chromatograph/mass spectrometer tests of the nonmetalized fuels, using a flash-heating oven, indicated that the relative concentrations of the pyrolyzed species depended strongly on temperature. For pure HTPB seven major products were identified, with 1,3-butadiene representing the dominant product at all temperatures tested, up to 1073 K. The measured mole fractions of the pyrolysis products and deduced pyrolysis laws of the fuels studied can be utilized in a comprehensive model simulation for combustion performance predictions.

Introduction

THE thermal pyrolysis of solid polymeric fuels is considered to be the rate-controlling step in the overall combustion process that takes place in hybrid-rocket motors and solid-fuel ramjet engines. Detailed knowledge of the response of the fuel surface to intense heating is imperative to the formulation and successful development of analytical modeling and prediction of combustion processes. Chemical kinetic parameters of the pyrolysis process, physical and chemical factors affecting fuel decomposition, the rate-controlling steps in the various stages of decomposition, and the identification and quantification of pyrolysis products are of special interest for the validation of combustion models and predictive codes.

Because of its importance to the combustion modeling of solid fuels and propellants, the pyrolysis of polymeric fuels/binders has been the subject of numerous studies over the past 40 years. The thermal decomposition of polybutadiene-based polymers (PBDs), and more specifically carboxyl- and hydroxyl-terminated polybutadienes (CTPB and HTPB, respectively), has received considerable attention since their emergence as prominent and widely used baseline binders/fuels in solid-propellant and hybrid-rocket motors about 25 years ago. Brief reviews of some research methods, experimental techniques, and pyrolysis mechanisms have been presented by McAlevy III and Blazowski,[1] Beck,[2] and Lengellé et al.[3]

An important aspect of solid-fuel pyrolysis research is the fuel sample heating rate. Bulk pyrolysis studies usually employ thermoanalytical methods such as thermogravimetric analysis (TGA), differential thermal analysis (DTA), and differential scanning calorimetry (DSC), conducted on very small fuel samples at low heating rates (in the range of 1–100°C/min). Data obtained by these thermal analysis techniques, sometimes in combination with mass spectrometry (MS) and gas chromatography (GC), allow the study of fuel degradation kinetics and the identification and quantification of pyrolysis products. Using these techniques, it is possible to determine the onset of thermal decomposition, Arrhenius parameters (activation energy E_a and pre-exponential factor A), and pyrolysis exothermicity/endothermicity as functions of the heating rate in the range mentioned.[4–14] The major disadvantages of these techniques are the use of very small material samples and low heating rates, which raise questions about the validity of extrapolating the data obtained to real combustion situations with heating rates several orders of magnitude higher.[12,15–18] In addition, at low heating rates slow low-temperature cooking reactions may proceed extensively, thus modifying the virgin material before the temperatures of interest are reached.[17,18] There are also serious doubts about the material homogeneity and temperature uniformity of the samples during the tests.[15,16]

The need to simulate more realistic conditions in laboratory tests, especially with respect to heating rates and real-time identification of the pyrolysis products, has prompted the development of the so-called thin-film or flash pyrolysis and linear or surface pyrolysis techniques. In the former method a very thin film of the solid-fuel material is deposited on electrically or radiatively heated metal ribbons or wires with heating rates on the order of 10^2–10^3°C/s (Refs. 13 and 17–22). Recently, Arisawa and Brill[21,22] have successfully developed and employed the T-jump/FTIR spectroscopy technique, which combines thin-film flash pyrolysis with near real-time infrared (IR) spectral detection. This procedure identifies the major gaseous pyrolysis products and their temperature- and

Received 12 April 1997; revision received 15 May 1998; accepted for publication 29 May 1998.

*Ph.D. Candidate, Department of Mechanical Engineering; currently Aerospace Engineer, Orbital Technologies Corporation, 1212 Fourier Drive, Madison, WI 53717. Member AIAA.
†Ph.D. Candidate, AFPL Palace Knight, Department of Mechanical Engineering. Member AIAA.
‡Research Associate, Department of Mechanical Engineering; currently Engineer, P.O. Box 97009, Primex Aerospace Company, 11441 Willows Road N.E., Redmond, WA 98073-9709. Member AIAA.
§Distinguished Professor, Department of Mechanical Engineering. Fellow AIAA.
¶Visiting Professor, Department of Mechanical Engineering; on sabbatical from RAFAEL, P.O. Box 2250, (M1), 31021, Haifa, Israel. Associate Fellow AIAA.
**Hybrid Propulsion Engineer, Advanced Propulsion Systems. Member AIAA.
††Hybrid Propulsion Engineer, Advanced Propulsion Systems.

pressure-dependent quantification and kinetics. In the linear or surface pyrolysis techniques, the fuel-sample surface is subjected to high heat flux with heating rates on the order of 10^3–10^4°C/s. An Arrhenius-type functional relationship between the measured surface temperature and regression rate yields the kinetic parameters A and E_a. The various experimental methods differ by the type of energy source and mode of heat transfer to the surface, as follows: 1) hot-plate conductive heating[23–26]; 2) hot-wire conductive heating[23]; 3) rocket-motor exhaust convective heating[15,16]; 4) diffusion flame self-heating[27,28]; and 5) arc-image radiant heating.[29] The shortcomings of the hot-plate pyrolysis method have been pointed out by several researchers.[1,23,24,27–30]

Based upon many pyrolysis studies, it is widely accepted that the pyrolysis of polybutadiene polymers generally proceeds by a two-stage mechanism. In the first stage starting at about 350°C, polymer depolymerization, cyclization, and crosslinking take place, accompanied by partial decomposition of the cyclized product. Heating-rate-dependent competition between depolymerization and cyclization has been revealed by several researchers.[5,6,11] In the second pyrolysis stage decomposition of the cyclized product occurs with increasing temperature, while depolymerization and cyclization reactions gradually disappear.[5,6,11] Extensive thermoanalytical studies of HTPB pyrolysis conducted by Zhang,[10] Du,[11] Chen and Brill,[13] and Lu and Kuo[14] show that the first pyrolysis stage is net exothermic, whereas the second pyrolysis stage is net endothermic for both HTPB resin and cured HTPB.

Using pyrolysis gas chromatography with mass spectral analysis in the thermal-decomposition study of cis-1,4 PBD, Radhakrishan and Rama Rao[8] have identified as many as 66 chromatograph peaks of volatile pyrolysis products with fragments as large as $C_{16}H_{26}$. Arisawa and Brill[21] recently reported the identification and quantification of 13 pyrolysis products (6 major and 7 minor) during flash pyrolysis of HTPB in a cool, static argon atmosphere, using thin-film samples of about 0.2 mg. The effect of pyrolysis temperature and pressure on the concentration of some major species was found to be significant.

Sensitivity studies of the effect of heating rate, sample size, pressure, and composition of the ambient gas mixture upon the thermal pyrolysis characteristics of solid fuels and binders have been conducted by many researchers. The significant effect of the heating rate on the energetics, degradation rate, and the Arrhenius-type kinetic parameters has been observed for all types of pyrolysis techniques.[2,5,9,16,18,25,27,31,32] Limited testing at pressures lower and higher than atmospheric did not reveal an appreciable effect of pressure in an inert atmosphere.[17,25,29] However, Arisawa and Brill[21] reported a significant change with pressure in the mole fraction of some major HTPB flash-pyrolysis products for tests in argon at pressure levels of 2 and 11 atm. Reported solid-fuel pyrolysis testing supports an observation that polymer pyrolysis in a reactive environment could be very different from decomposition in an inert environment, depending upon the type of fuel and oxidizing species. This observation may be especially relevant when pyrolysis is conducted at higher than atmospheric pressure.[2,15–18,29] These conditions are of special interest to hybrid propulsion.

The major objectives of the present study are as follows: 1) to characterize the pyrolysis behavior of four solid-fuel formulations, suitable for hybrid rocket applications, with respect to surface temperature at high heating rates characteristic of real hybrid motors; 2) to provide experimental pyrolysis data in terms of regression rates, Arrhenius parameters, and subsurface temperature profiles as a function of surface temperature for model simulation and validation; 3) to identify and quantify the major pyrolysis products of the nonmetalized fuels at various temperatures, and 4) to acquire a better understanding of the pyrolysis mechanisms of the solid fuels.

The fuels studied in this investigation included pure HTPB, designated SF1, 80% HTPB/20% ultra-fine activated aluminum powder,[33] designated SF2, 80% HTPB/20% conventional aluminum powder, designated SF3, and the Joint Industrial Research and Development (JIRAD) fuel formulation,[34] designated SF4. The ultrafine aluminum powder (also called Alex) used in this study was manufactured via a plasma explosion process and had a mean particle size range of 0.05–0.10 μm. The conventional aluminum powder had a mean particle size of 5–15 μm.

Method of Approach

To test solid fuels under the high heating rate conditions encountered in practical hybrid rocket motors (on the order of 1000°C/s), a hot-cylinder conductive heating method was used to pyrolyze the solid-fuel samples. The samples had a typical diameter of 6 mm and length of 20 mm. For each test a fuel sample was placed in a sealed, windowed pyrolysis chamber. Figure 1 shows a schematic diagram of the conductive heating test facility, including the windowed test chamber, tube furnace, and ball valves. Most tests were conducted at atmospheric pressure in a nitrogen environment. A hot copper cylinder was preheated in a tube furnace situated above the pyrolysis chamber and then dropped onto the fuel sample to initiate and sustain thermal pyrolysis. The cylinder was 12.7 mm in diameter and 76 mm in length. Copper was chosen as the cylinder material for its combination of high thermal conductivity and large volumetric heat capacity. The cylinder had a selected initial uniform temperature in the range of 800–1300 K. During the heating period in the furnace, the copper cylinder was held at the end of a suction tube connected to a vacuum pump. Two chromel/alumel K-type thermocouples were used to measure precisely the controlled ambient gas temperature near the copper cylinder inside the furnace. When the desired cylinder temperature at equilibrium was reached, a three-way ball valve was activated to switch the suction tube pressure from partial vacuum to atmospheric pressure, thus causing the cylinder to fall through the feeding tube system onto the fuel sample, as shown in Fig. 2. A dual ball-valve system served as an airlock, allowing the chamber to remain pressurized during the cylinder dropping process (see Fig. 1). During this interval, the cylinder first fell out of the furnace, through the upper ball valve (normally open) and onto the lower ball valve (normally closed). The upper ball valve was then closed, and the lower ball valve opened to allow the cylinder to land on the fuel sample.

The conductive-heating chamber was instrumented with a number of diagnostic devices. A fine-wire thermocouple (25-μm junction size) was embedded in the solid-fuel strand to measure the subsurface temperature profile and instantaneous surface temperature. The thermocouple was soldered to extension posts mounted on the diagnostic ring, as shown in Fig. 2. The thermocouple provided instant measurements of the cylinder/fuel interface temperature when the interface reached the thermocouple location and thereafter by traveling downward with the surface.

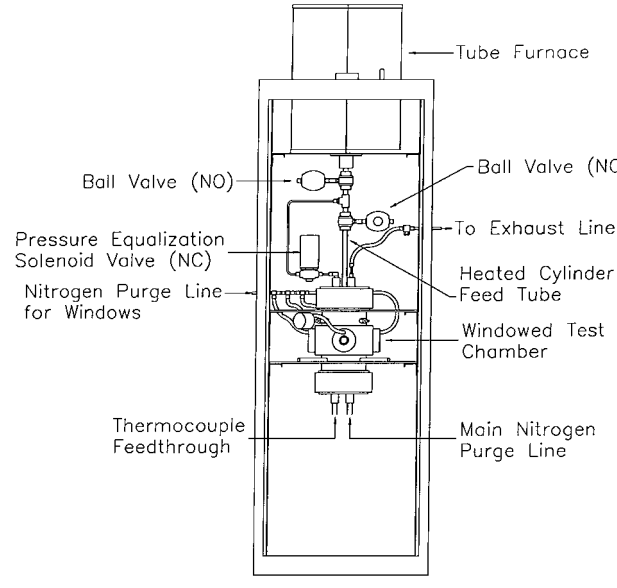

Fig. 1 Layout of the conductive-heating fuel pyrolysis experimental setup.

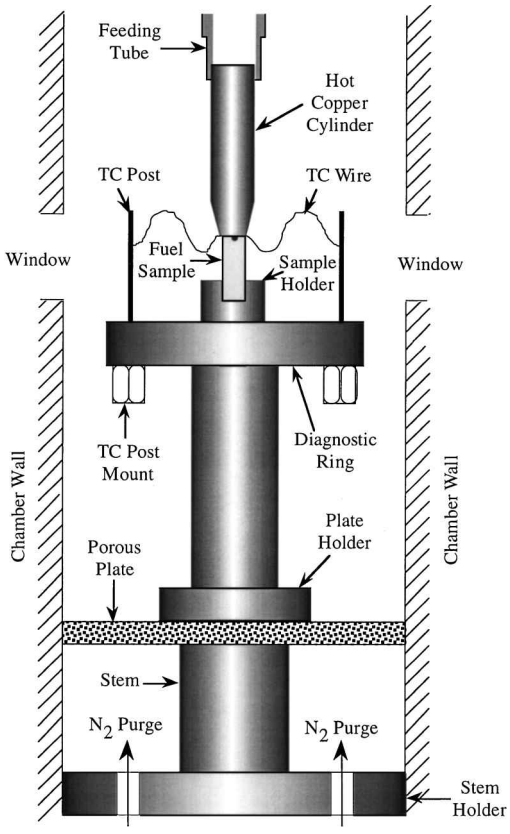

Fig. 2 Solid-fuel sample heated by hot metal cylinder.

The pyrolysis process was observed using a high-resolution Pulnix video camera at 60 frames/s. Video images were recorded on videotape and analyzed with image processing software on a personal computer. The instantaneous regression rate was deduced by tracking the movement of the cylinder/fuel interface over the test duration. During each test, a nitrogen purge was activated to carry the pyrolysis products into the exhaust system and thereby prevent the deposition of products on the transparent viewing windows. A perforated plate distributed the purge gas evenly around the sample. Each window also had an individual nitrogen purge to maintain a clear view of the pyrolysis process. A Setra pressure transducer was used to measure chamber pressure-time variations during the tests. The chamber was purged and pressurized with nitrogen during each test to provide an inert environment for study of the pyrolysis process. The purge rate was measured using an Omega electronic mass flow meter.

A series of TGA and DTA tests were performed for the SF1 and SF4 fuels. The objective of these tests was to gain insights into the thermal behavior of the fuels. During the TGA tests, a small amount of fuel was heated from ambient temperature to 800°C (1073 K) at 5°C/min, while during the DTA tests the sample was heated to 1300°C (1573 K), also at 5°C/min. Nitrogen was used as the purge gas.

The identification and quantification of pyrolyzed species from the solid fuel was accomplished using a Shimadzu QP-5000 GC/MS system, coupled with a Shimadzu PYR-4A high-temperature pyrolyzer. The GC/MS system can scan an atomic mass range of up to 800 amu at a maximum scanning rate of 6000 amu/s. The chemical compounds in the pyrolyzed gas mixture were separated using a 100 m long, 0.25-mm diam Supelco-made Petrocol DH capillary column.

To perform these tests, a small sample of solid fuel (0.12–1.0 mg) was placed in the oven of the PYR-4A pyrolyzer, which was maintained at a preset pyrolysis temperature (800°C maximum). The solid-fuel sample then underwent flash pyrolysis. The heating rate of the flash pyrolysis process was equivalent to that experienced by the solid-fuel samples tested in the conductive heating experiments and was considered to be similar to those of hybrid motor firing conditions. A helium carrier gas then delivered the pyrolysis products directly into the capillary column for species separation and afterward into the mass spectrometer for ionization, fragmentation, and detection. The nonmetalized solid-fuel formulations, SF1 and SF4, were each tested at 500, 600, 700, and 800°C, to study the effect of temperature on the relative product concentration. The aluminized fuel formulations were not tested with this system as they contained metal particles that can clog the capillary tube and/or damage the GC/MS electronics.

Chemical species identification was accomplished by comparing the detected mass spectrum of each chromatograph peak to a library database. To quantify the identified species, known quantities of liquid and gaseous pure substances were injected into the GC/MS system to determine the calibration factors of individual species. The concentration of each species in the pyrolysis mixture was then obtained by comparing the area of its chromatograph peak with the corresponding calibration factor obtained using the pure substance.

Discussion of Results

Regression-Rate Measurements

The solid-fuel regression rates r were deduced by analyzing real-time video images of the pyrolyzing fuel strands. The image processing software was typically used to capture six to seven images per second. Because the regression-rates were usually less than 1 mm/s, this capture rate provided sufficient temporal resolution to determine the regression rate.

Figure 3 shows a plot of the trajectories of the cylinder/fuel interface for three different cases of HTPB pyrolysis in a nitrogen environment at atmospheric pressure. The regression rates were deduced by curve fitting the interface position-time traces and then taking the time derivatives of the resulting equations. Because the regression rates appeared to be quite constant with respect to the test time for a given initial cylinder temperature, linear functions were used to fit the data. The constant nature of the deduced regression rates indicates that the surface temperature remained approximately constant throughout the test. Note that the indicated temperatures for these data correspond to the initial cylinder temperature ($T_{\mathrm{cyl},i}$) and not to the measured fuel surface temperature. As expected, the test conducted with the highest initial cylinder temperature of 1000 K displayed the fastest regression rate, 0.57 mm/s. For initial cylinder temperatures of 900 and 800 K, the deduced regression-rates were 0.42 and 0.13 mm/s, respectively. The error of the regression-rate measurements was estimated to be within ±1% of the deduced value.

Surface-Temperature Measurements

Figure 4 displays a typical temperature-time trace for solid-fuel SF1 obtained using the embedded thermocouple technique. Before it sensed the approaching hot cylinder, the embedded thermocouple indicated an ambient temperature of about 300 K. As the copper cylinder caused the fuel strand to start pyrolyzing and regressing

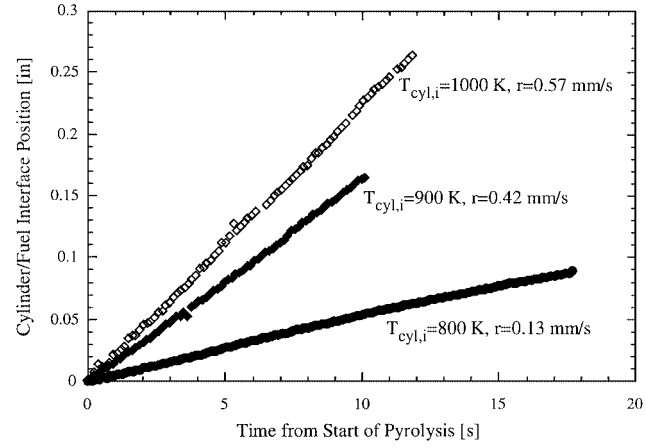

Fig. 3 Cylinder/fuel interface trajectory for SF1 thermal pyrolysis.

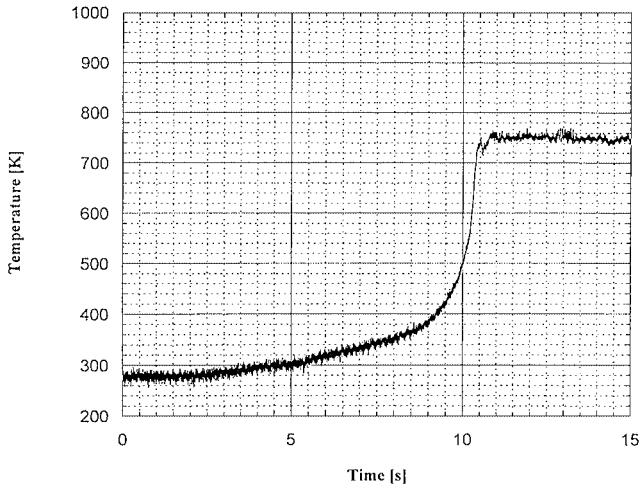

Fig. 4 Typical temperature-time trace for solid fuel SF1.

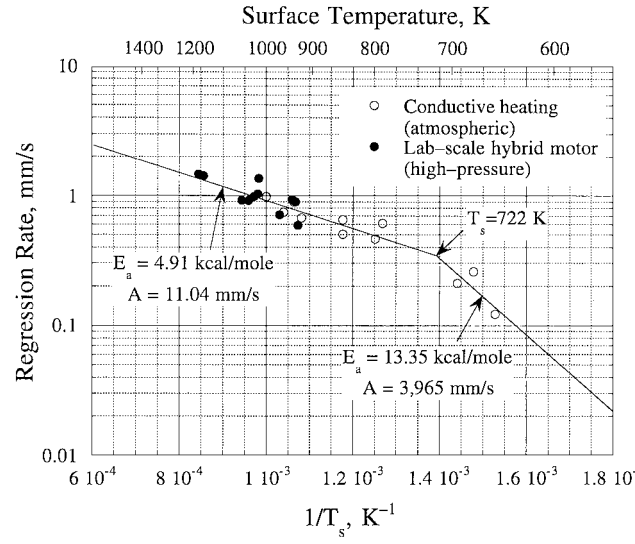

Fig. 5 Arrhenius-type plot for the pyrolysis of solid fuel SF1.

downward, the thermocouple registered a continuous temperature increase. About 8 s after the start of the temperature rise, a peak temperature of 760 K was reached. This peak temperature corresponds to the deduced surface temperature. At this point the cylinder/fuel interface reached the location of the embedded thermocouple, and the thermocouple began to move downward with the regressing fuel surface. The thermocouple continued to register the surface temperature for the remainder of the test. The error of the surface temperature measurements was estimated to be within $\pm 1.2\%$ of the deduced value.

The temperature-time trace shown in Fig. 4 exhibits a steep gradient near the pyrolyzing fuel surface, corresponding to a heating rate of about 1100°C/s. This heating rate value is representative of that expected in large-scale hybrid motors.[3] Notice that the surface temperature of 760 K remained relatively constant, implying that the copper cylinder had sufficient thermal inertia to supply continuously the required thermal energy necessary to pyrolyze the solid fuel without noticeable surface temperature decay. This finding suggests that the thermal response time of the fuel, which can be expressed as the ratio of the thermal diffusivity to the square of the regression rate (α/r^2) is relatively short compared with the time required for the surface temperature to change by any significant amount (for example, on the order of 10 K).

Deduced Solid-Fuel Pyrolysis Laws

Using the deduced regression rates and surface temperatures, Arrhenius-type pyrolysis laws were obtained for each of the four fuel formulations tested. Figure 5 shows the Arrhenius plot for HTPB (SF1) in terms of regression rate (in mm/s) vs the reciprocal of the surface temperature, $1/T_s$ (in K^{-1}). The top axis shows the corresponding surface temperature.

Atmospheric pressure data from the present conductive-heating tests (closed circles) and high-pressure (375–600 psi) data from hybrid motor tests (open circles)[35] were both used to deduce the pyrolysis law for HTPB. Reference 35 provides a detailed description of the lab-scale hybrid motor used in a recent investigation to obtain the regression rate and surface temperature data. At surface temperatures higher than 722 K, both sets of data follow the same trend and fit reasonably well to a single straight line on the semilog plot represented by the Arrhenius-type expression

$$r = A \exp(-E_a/R_u T_s) \tag{1}$$

or

$$\ln(r) = \ln(A) - E_a/R_u T_s \tag{2}$$

where $E_a = 4.91$ kcal/mol, $A = 11.04$ mm/s, and R_u is the universal gas constant (kcal/mol-K). At temperatures below 722 K, the data follow another trend, with $E_a = 13.35$ kcal/mol and $A = 3965$ mm/s. Equation (1) is given strictly in the Arrhenius form instead of the pyrolysis law based upon bulk kinetics:

$$r = A \exp(-E_{py}/2R_u T_s) \tag{3}$$

where E_{py} has twice the value of E_a. The bulk pyrolysis rate usually corresponds to the activation energy based on E_{py} instead of E_a. Arisawa and Brill[22] have recently obtained a relatively low activation energy (E_{py}) of 12 kcal/mol for HTPB under high heating rates of about 600°C/s at a pressure of 11 atm and temperature range of 460–600°C. Arisawa and Brill[21,22] have stated that low activation energies (such as those cited here) indicate that the overall pyrolysis process is limited by physical desorption of pyrolyzed fuel molecules from the solid-fuel surface, and not by chemical processes, such as polymer chain scission and cyclization, in the solid-fuel decomposition zone just below the surface. The latter are characterized by higher activation energies (E_{py}) on the order of 40–50 kcal/mol and dominate the pyrolysis process at low heating rates or low surface temperatures. This difference in mechanisms may explain why Lu and Kuo[14] found a higher E_{py} at very low heating rates using thermal analysis tests (TGA, DTA, DSC). The low-temperature test data (below 722 K) obtained in this study correspond to lower activation energies than those of conventional thermal analysis tests.

The comparison of high-pressure and atmospheric pressure test data shown in Fig. 5 suggests that there is no significant effect of pressure on the HTPB Arrhenius parameters for the surface-temperature range tested. In addition, the conductive-heating regression-rate data matched well with the hybrid motor data, which indicates that the conductive-heating method can adequately simulate motor test firing conditions. This agreement also implies that the net energy feedback from the diffusion flame in the hybrid motor situation is similar to the heat-transfer rate from the hot metal cylinder. In both cases the solid fuel regression rate is governed by the magnitude of the surface temperature.

Figure 6 shows the superimposed pyrolysis results of the conductive-heating pyrolysis tests for both HTPB (SF1) and the metalized fuels (SF2 and SF3), as well as the results of the lab-scale hybrid motor tests for SF1. As clearly indicated, the addition of neither the Alex powder[33] nor the conventional aluminum powder affected the Arrhenius parameters of pure HTPB in the present study. However, results from the previous hybrid combustion study on solid-fuel regression rates in a lab-scale motor indicated that the addition of 20 wt% Alex powder to HTPB increased the fuel mass burning rate $\rho_f r$ by 70% and the regression rate r by 43.8% over that of pure HTPB at the same operating conditions.[35] The Alex powder in the SF2 fuel formulation did not influence the regression rate in the conductive-heating induced pyrolysis tests. This difference in behavior between the conductive-heating tests and the hybrid

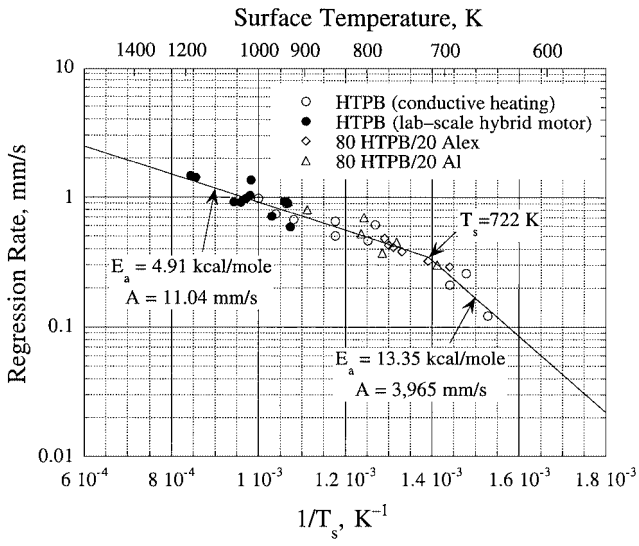

Fig. 6 Comparison of solid fuels SF1, SF2, and SF3.

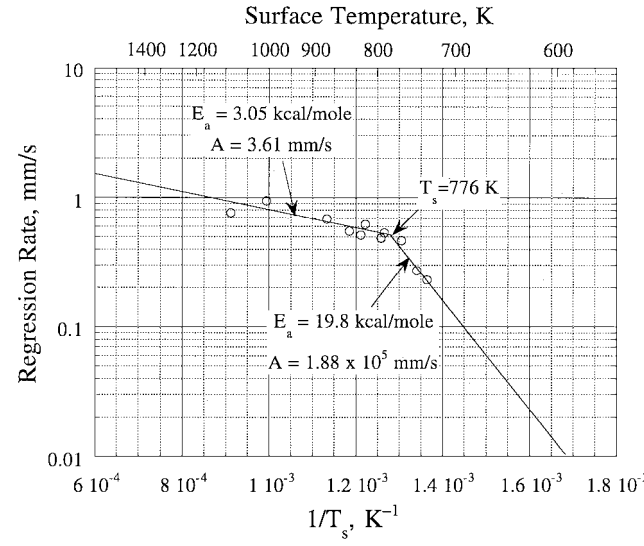

Fig. 7 Arrhenius-type plot for the pyrolysis of solid fuel SF4.

motor firings could be explained by the different test conditions imposed on the fuel surface. When the SF2 fuel had a free surface to react, as in the hybrid motor experiments, the exothermic heat release induced by the Alex additive was very pronounced. In the conductive-heating tests close physical contact with the heated metal cylinder may have suppressed the effect of the exothermic reaction of the Alex powder. On the recorded video images of the fuel sample pyrolysis event, some luminous flamelets were observed near the outer edge of the interface between the metal cylinder and fuel. These luminous flamelets were observed only for SF2 (not SF3), indicating the existence of a nonoxidative, exothermic heat-release process associated with the presence of Alex particles. However, these heat-release zones could not directly contribute to the heat feedback to the unpyrolyzed solid fuel because of the presence of the metal cylinder. The metal cylinder may have acted as a heat sink to absorb any local exothermic heat release caused by the Alex. This explains why the regression rates of SF2 fuel follow the same trend in the conductive heating-induced pyrolysis experiments as SF1.

A measured 12% increase in the lab-scale hybrid motor regression rate associated with the addition of 20% conventional aluminum[35] is most likely caused by enhanced radiant heat flux from metalized combustion products and possibly also by increased flame temperature. These effects were not present during the conductive-heating pyrolysis tests; therefore, the addition of conventional aluminum powder did not affect the regression rates of the solid-fuel samples during the present study.

Figure 7 shows the Arrhenius plot for the JIRAD fuel formulation (SF4). SF4 also displayed two sets of parameters, with a transition temperature of 776 K. At surface temperatures below 776 K, $E_a = 19.8$ kcal/mol and $A = 1.88 \times 10^5$ mm/s, whereas above this temperature $E_a = 3.05$ kcal/mol and $A = 3.61$ mm/s. Again, in the low-temperature regime the pyrolysis process is believed to be dominated by chemical processes that require higher E_a, whereas physical desorption determines the regression rate in the high-temperature regime. SF4 was not tested in the lab-scale hybrid motor, and the authors are not aware of any other surface temperature data available for this fuel formulation besides the measurements made in this study. Therefore, no comparisons could be made between motor firing data and the conductive-heating data for the JIRAD solid fuel.

Thermal Analysis of SF1 and SF4

The TGA tests indicated that SF1 began to show significant weight loss around 300°C. The TGA trace for SF1 can be found in Ref. 14. On the other hand, SF4 showed noticeable weight loss at a lower temperature (150°C). This behavior is probably caused by the decomposition of polycyclopentadiene (Escorez 5320) in SF4 (Ref. 34).

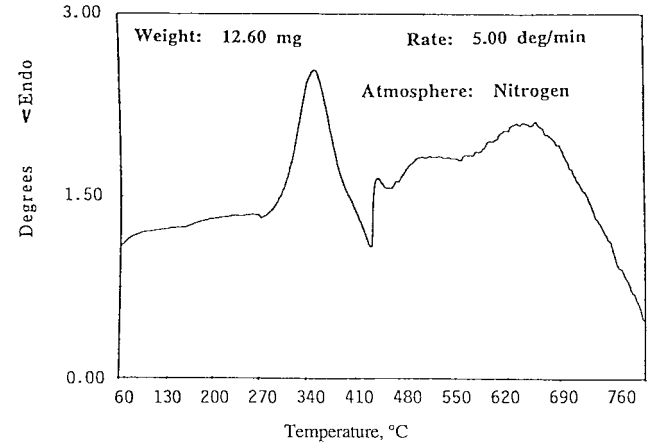

Fig. 8a DTA trace of solid fuel SF1.

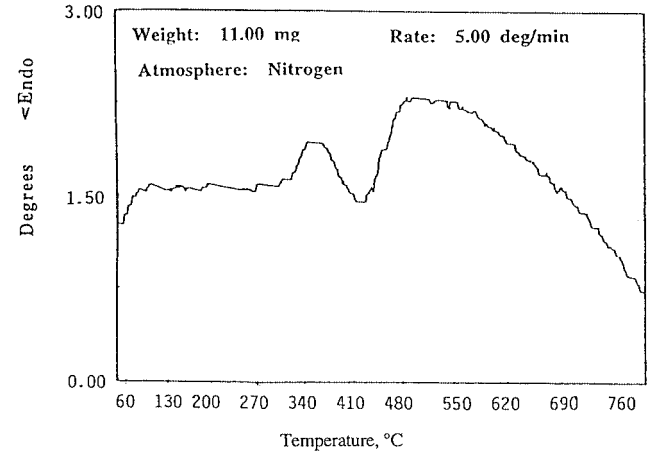

Fig. 8b DTA trace of solid fuel SF4.

The DTA tests show initial exotherms followed by endotherms for both the SF1 and SF4 formulations. Although the exotherms and endotherms of these two fuels occur at the same temperatures, the magnitudes of the peaks and valleys are different, as shown in Figs. 8a and 8b. It is believed that cyclization and crosslinking reactions cause the exothermic process, whereas the endothermic process is caused by depolymerization and decomposition reactions.

Table 1 Major pyrolysis products of pure HTPB (SF1) and their relative molar concentrations at various temperatures

Major pyrolysis product species (M_i), chemical formula	Relative molar concentration of pyrolysis products at various temperatures, %			
	500°C	600°C	700°C	800°C
Ethene, C_2H_4	——	5.59	3.05	6.58
Propene, C_3H_6	——	——	4.90	10.99
1,3-Butadiene, C_4H_6	77.4	89.06	66.1	41.07
3-Pentene-1-yne, C_5H_6	——	——	9.20	10.28
Benzene, C_6H_6	——	——	10.3	22.02
Toluene, C_7H_8	——	——	6.41	9.06
4-Vinyl-cyclohexene, C_8H_{12}	22.6	5.35	——	——

Table 2 Major pyrolysis products of JIRAD fuel (SF4) and their relative molar concentrations at various temperatures

Major pyrolysis product species (M_i), chemical formula	Relative molar concentration of pyrolysis products at various temperatures, %			
	500°C	600°C	700°C	800°C
Ethene, C_2H_4	——	12.65	14.49	29.93
Propene, C_3H_6	——	4.56	7.38	11.94
1,3-Butadiene, C_4H_6	78.70	53.36	44.70	11.05
3-Pentene-1-yne, C_5H_6	——	11.29	18.36	14.27
Cyclopentene, C_5H_8	——	3.92	——	——
Benzene, C_6H_6	——	4.89	10.41	13.63
Toluene, C_7H_8	——	——	4.66	5.22
4-Vinyl-cyclohexene, C_8H_{12}	21.30	9.33	——	——
Styrene, C_8H_8	——	——	——	2.49
Indene, C_9H_8	——	——	——	6.04
Naphthalene, $C_{10}H_8$	——	——	——	5.43

Pyrolysis Product Identification and Quantification

To identify and quantify the solid-fuel pyrolysis products under realistic heating rates, pure HTPB (SF1) and the JIRAD fuel formulation (SF4) were pyrolyzed using the GC/MS oven. The GC/MS pyrolysis tests indicated that the relative concentrations of the major decomposition products depended very strongly upon the pyrolysis temperature. The generalized equation for a solid fuel to decompose into n chemical species can be written as

$$\text{Solid} \cdot \text{Fuel} \cdot \rightarrow \sum_{i}^{n} X_i M_i \tag{4}$$

where X_i represents the relative molar concentration of species M_i. The identity of each of the major pyrolysis products M_i and its corresponding value of X_i are given in Tables 1 and 2 for SF1 and SF4, respectively.

Figures 9a and 9b show the total ion chromatogram (TIC) of the pyrolysis products generated from pure HTPB as these products were separated and detected by the GC/MS system at pyrolysis temperatures of 500 and 800°C, respectively. Two major chemical species, 1,3-Butadiene (BD) and 4-Vinyl-Cyclohexene (VCH), appeared during the 500°C test. Numerous fragmented species evolved at 800°C.

Table 1 lists the identity and corresponding molar concentrations of each of the major pyrolysis products at four different temperatures. Several of these species have been observed by Arisawa and Brill.[21] According to Table 2, 1,3-BD had a concentration of about 3.4 times that of 4-VCH at 500°C. As the pyrolysis temperature increased to 600°C, where BD had its largest concentration, the amount of 4-VCH relative to that of BD decreased. Ethene (ET) became a noticeable product, with a concentration similar to that of 4-VCH at this temperature. At 700°C, 4-VCH was no longer detectable, and the relative concentration of BD, still the most abundant species, dropped below its values at the lower temperatures. Propene (PR), 3-Pentene-1-Yne (PT), Benzene (B), and Toluene (T) became important species at 700°C, having much larger concentrations than

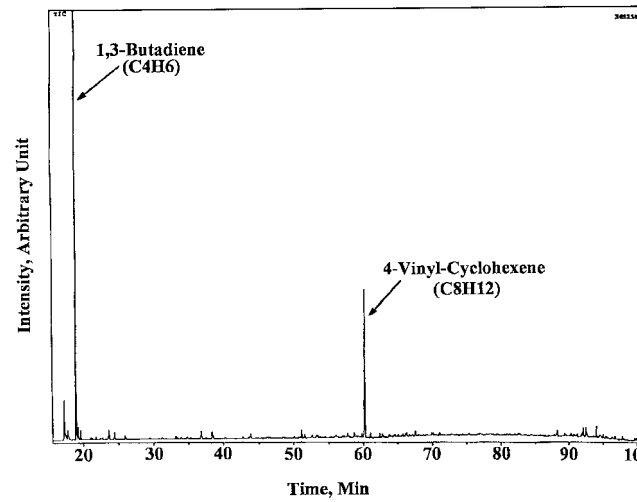

Fig. 9a Total ion chromatogram of pyrolysis products generated from solid fuel SF1 at 500°C.

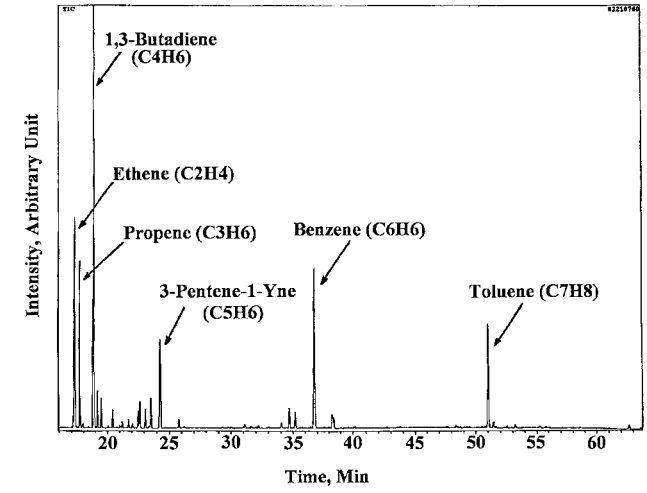

Fig. 9b Total ion chromatogram of pyrolysis products generated from solid fuel SF1 at 800°C.

at lower temperatures. At the maximum pyrolysis temperature used, 800°C, six major species were detected: BD, ET, B, PR, T, and PT. While the relative concentration of BD again decreased, the other major species became more abundant.

HTPB was also pyrolyzed at 300 and 400°C using the GC/MS system and pyrolyzing oven. At these temperature levels evaporation of the curing agent Isonate 143 L was the major process. At 400°C a very small amount of 4-VCH was also detected. Most of the solid-fuel samples were left in the sample holder as residue during these tests, suggesting that the threshold pyrolysis temperature of HTPB is between 400–500°C.

Table 2 shows the pyrolysis products of the JIRAD fuel formulation at four different temperatures. In contrast to the results for pure HTPB, ET had the highest concentration at 800°C, nearly 30%, whereas PR, PT, and B all had concentrations similar to that of 1,3-BD at this temperature. Species with eight or more carbon atoms (such as Styrene, Indene, and Naphthalene) contributed together almost 14% of the major species at 800°C. The concentration of T in SF4 did not vary significantly with a temperature increase from 700 to 800°C. One of the species detected from this fuel at 600°C matched very well with the mass spectrum pattern of Isophorone diisocyanate (IPDI).

The data shown in Tables 1 and 2, combined with the Arrhenius parameters and regression-rate law in the form of Eq. (1), can be used to specify the rate of production of pyrolyzed species from the fuel surface by equating the surface temperature to the

pyrolysis temperature. This information is necessary for comprehensive model simulation of solid-fuel combustion processes in hybrid rocket motors. Knowing mole fractions of the pyrolysis products generated from the fuel surface, one can model the gas-phase reaction kinetics and calculate the transport properties required for detailed numerical simulation and performance calculations.

Conclusions

A hot-cylinder conductive-heating technique was successfully developed and employed to determine Arrhenius parameters for the thermal pyrolysis of four solid fuels under high heating-rate conditions. Thermal analysis methods (TGA and DTA) were applied to study the decomposition characteristics and energetics of the pyrolysis of HTPB (SF1) and JIRAD (SF4) fuels. The major pyrolysis products of SF1 and SF4 were identified and quantified as functions of pyrolysis temperature using a GC/MS system with a pyrolyzing oven.

Several conclusions can be drawn from the results of this study:

1) The conductive-heating induced pyrolysis rates of HTPB (SF1), obtained in an inert environment, were consistent with those measured previously during lab-scale hybrid motor firings. This result implies that the solid-fuel regression rate of HTPB in hybrid motors operating under realistic conditions is governed primarily by thermal decomposition processes in the fuel surface region.

2) The solid-fuel activation energies (E_a) were found to depend strongly on surface temperature, but not on pressure. At low surface temperatures the E_a values were higher because the pyrolysis processes were dominated by the chemical processes of depolymerization, cyclization, and crosslinking. At high surface temperatures the E_a values were lower because physical desorption of large polymer fragments from the fuel surface represented the rate-limiting mechanism.

3) Mole fractions of the solid-fuel pyrolysis products depended strongly on temperature. At relatively low temperatures (around 500°C) the major pyrolysis products were 1,3-BD and 4-VCH for both HTPB and the JIRAD fuel. At relatively high temperatures (around 800°C) 1,3-BD became less dominant, but still represented the largest mole fraction of decomposed species from HTPB. For the JIRAD fuel ET had the largest mole fraction at 800°C.

4) In conductive-heating-induced tests the addition of aluminum powder to HTPB did not alter the Arrhenius parameters. This result is believed to be caused by the heat-sink effect of the copper cylinder in the absorption of any localized exothermic heat release from the presence of Alex or conventional aluminum additive.

The thermal pyrolysis data obtained in this study should be very useful for detailed modeling of combustion processes and performance calculations for hybrid rocket propulsion systems.

Acknowledgments

The authors wish to thank Lockheed Martin Manned Space Systems for funding this work. The assistance of Michael Gregorchik and Christine Mineo in the conduction of the thermal pyrolysis tests is greatly appreciated. We would also like to thank Roger Harwell of NASA Marshall Space Flight Center for authorizing the supply of the JIRAD fuel samples to Pennsylvania State University.

References

[1]McAlevy, R. F., III, and Blazowski, W. S., "The Surface Pyrolysis Boundary Condition for the Combustion of Polymers," *Proceedings of the 4th Materials Research Symposium*, edited by L. A. Wall, NBS Special Publ. 357, U.S. Government Printing Office, Washington, DC, 1972, pp. 185–192.

[2]Beck, W. H., "Pyrolysis Studies of Polymeric Materials Used as Binders in Composite Propellants: A Review," *Combustion and Flame*, Vol. 70, No. 2, 1987, pp. 171–190.

[3]Lengellé, G., Fourest, B., Godon, J. C., and Guin, C., "Condensed Phase Behavior and Ablation Rate of Fuels for Hybrid Propulsion," AIAA Paper 93-2413, June 1993.

[4]Varney, A. M., and Strahle, W. C., "Thermal Decomposition Studies of Some Solid Propellant Binders," *Combustion and Flame*, Vol. 16, No. 1, 1971, pp. 1–8.

[5]Brazier, D. W., and Schwartz, N. V., "The Effect of Heating Rate on the Thermal Degradation of Polybutadiene," *Journal of Applied Polymer Science*, Vol. 22, No. 1, 1978, pp. 113–124.

[6]McCreedy, K., and Keskkula, H., "Effect of Thermal Crosslinking on Decomposition of Polybutadiene," *Polymer*, Vol. 20, No. 8, 1979, pp. 1155–1159.

[7]Thomas, T. J., and Krishnamurthy, V. N., "Thermogravimetric and Mass-Spectrometric Study of the Thermal Decomposition of PBCT Resins," *Journal of Applied Polymer Science*, Vol. 24, No. 8, 1979, pp. 1797–1808.

[8]Radhakrishnan, T. S., and Rama Rao, M., "Thermal Decomposition of Polybutadienes by Pyrolysis Gas Chromatography," *Journal of Polymer Science: Polymer Chemistry Edition*, Vol. 19, No. 12, 1981, pp. 3197–3208.

[9]Ninan, K. N., and Krishnan, K., "Thermal Decomposition Kinetics of Polybutadiene Binders," *Journal of Spacecraft and Rockets*, Vol. 19, No. 1, 1982, pp. 92–94.

[10]Zhang, D., "Systematic Studies on Thermal Decomposition of Hydroxy-Terminated Polybutadiene (HTPB)," International Astronautical Federation, Preprint IAF-ST-88-05, Oct. 1988.

[11]Du, T., "Thermal Decomposition Studies of Solid Propellant Binder HTPB," *Thermochimica Acta*, Vol. 138, No. 2, 1989, pp. 189–197.

[12]Rama Rao, M., and Radhakrishnan, T. S., "Thermal Degradation of Functionally Terminated Polybutadienes: Pyrolysis Gas Chromatography and Thermogravimetric Studies," *Journal of Applied Polymer Science*, Vol. 41, Nos. 9 and 10, 1990, pp. 2251–2263.

[13]Chen, J. K., and Brill, T. B., "Chemistry and Kinetics of Hydroxyl-Terminated Polybutadiene (HTPB) and Diisocyanate—HTPB Polymers During Slow Decomposition and Combustion-Like Conditions," *Combustion and Flame*, Vol. 87, Nos. 3 and 4, 1991, pp. 217–232.

[14]Lu, Y.-C., and Kuo, K. K., "Thermal Decomposition Study of Hydroxyl-Terminated Polybutadiene (HTPB) Solid Fuel," *Thermochimica Acta*, Vol. 275, No. 2, 1996, pp. 181–191.

[15]McAlevy, R. F., III, and Hansel, J. G., "Linear Pyrolysis of Thermoplastics in Chemically Reactive Environments," *AIAA Journal*, Vol. 3, No. 2, 1965, pp. 244–249.

[16]Hansel, J. G., and McAlevy, R. F., III, "Energetics and Chemical Kinetics of Polystyrene Surface Degradation in Inert and Chemically Reactive Environments," *AIAA Journal*, Vol. 4, No. 5, 1966, pp. 841–848.

[17]Cheng, J. T., Ryan, N. W., and Baer, A. D., "Oxidative Decomposition of PBAA Polymer at High Heating Rates," *Proceedings of the Twelfth International Symposium on Combustion*, edited by M. W. Evans, The Combustion Institute, Pittsburgh, PA, 1969, pp. 525–532.

[18]Bouck, L. S., Baer, A. D., and Ryan, N. W., "Pyrolysis and Oxidation of Polymers at High Heating Rates," *Proceedings of the Fourteenth (International) Symposium on Combustion*, edited by J. P. Longwell, The Combustion Institute, Pittsburgh, PA, 1973, pp. 1165–1176.

[19]Baer, A. D., Hedges, J. H., Seader, J. D., Jayakar, K. M., and Wojcik, L. H., "Polymer Pyrolysis over a Wide Range of Heating Rates," *AIAA Journal*, Vol. 15, No. 10, 1977, pp. 1398–1404.

[20]Brill, T. B., "Fast Thermolysis-Fourier Transform Infrared Spectroscopy Methods to Study Energetic Materials," *Chemistry and Physics of Energetic Materials*, edited by S. N. Bulusu, Kluwer Academic, Norwell, MA, 1990, pp. 255–276.

[21]Arisawa, H., and Brill, T. B., "Flash Pyrolysis of Hydroxyl-Terminated Polybutadiene (HTPB) I: Analysis and Implications of the Gaseous Products," *Combustion and Flame*, Vol. 106, Nos. 1 and 2, 1996, pp. 131–143.

[22]Arisawa, H., and Brill, T. B., "Flash Pyrolysis of Hydroxyl-Terminated Polybutadiene (HTPB) II: Implications of the Kinetics to Combustion of Organic Polymers," *Combustion and Flame*, Vol. 106, Nos. 1 and 2, 1996, pp. 144–154.

[23]Schultz, R. D., and Dekker, A. O., "The Absolute Thermal Decomposition Rates of Solids," *Proceedings of the Fifth International Symposium on Combustion*, edited by H. C. Hottel, The Combustion Institute, Pittsburgh, PA, 1955, pp. 260–267.

[24]Barsh, M. K., Andersen, W. H., Bills, K. W., Moe, G., and Schultz, R. D., "Improved Instrument for the Measurement of Linear Pyrolysis Rates of Solids," *Review of Scientific Instruments*, Vol. 29, No. 5, 1958, pp. 392–395.

[25]Chaiken, R. F., Andersen, W. H., Barsh, M. K., Mishuck, E., Moe, G., and Schultz, R. D., "Kinetics of the Surface Degradation of Polymethylmethacrylate," *Journal of Chemical Physics*, Vol. 32, No. 1, 1960, pp. 141–146.

[26]Chaiken, R. F., and Van de Mark, D. K., "Thermocouple Junction for a Hot-Plate Linear Pyrolysis Apparatus," *Review of Scientific Instruments*, Vol. 30, No. 5, 1959, pp. 375, 376.

[27]McAlevy, R. F., III, Lee, S. Y., and Smith, W. H., "Linear Pyrolysis of Polymethylmethacrylate During Combustion," *AIAA Journal*, Vol. 6, No. 6, 1968, pp. 1137–1142.

[28]Blazowski, W. S., Cole, R. B., and McAlevy, R. F., III, "Linear Pyrolysis of Various Polymers Under Combustion Conditions," *Proceedings of the Fourteenth International Symposium on Combustion*, edited by J. P. Longwell, The Combustion Institute, Pittsburgh, PA, 1973, pp. 1177–1186.

[29]Cohen, N. S., Fleming, R. W., and Derr, R. L., "Role of Binders in Solid Propellant Combustion," *AIAA Journal*, Vol. 12, No. 2, 1974, pp. 212–218.

[30]Nachbar, W., and Williams, F. A., "On the Analysis of Linear Pyrolysis Experiments," *Proceedings of the Ninth International Symposium on Combustion*, edited by W. G. Berl, The Combustion Institute, Pittsburgh, PA, 1963, pp. 345–357.

[31]Price, E. W., "Comment on 'Thermal Decomposition Kinetics of Polybutadiene Binders,'" *Journal of Spacecraft and Rockets*, Vol. 20, No. 3, 1983, p. 320.

[32]Chaiken, R. F., and Andersen, W. H., "The Role of Binder in Composite Propellant Combustion," *Solid Propellant Rocket Research*, edited by M. Summerfield, Vol. 1, Progress in Astronautics and Rocketry, Academic International Press, New York, 1960, pp. 227–249.

[33]Ivanov, G. V., and Tepper, F., "'Activated' Aluminum as a Stored Energy Source for Propellants," *Challenges in Propellants and Combustion 100 Years after Nobel*, edited by K. K. Kuo, Begell House, New York, 1997, pp. 634–643.

[34]Boardman, T. A., Carpenter, R. L., Goldberg, B. E., and Shaeffer, C. W., "Development and Testing of 11- and 24-inch Hybrid Motors Under the Joint Government/Industry IR&D Program," AIAA Paper 93-2552, June 1993.

[35]Chiaverini, M., Serin, N., Johnson, D. K., Lu, Y. C., and Kuo, K. K., "Instantaneous Regression Behavior of HTPB Solid Fuels Burning with GOX in a Simulated Hybrid Motor," *Challenges in Propellants and Combustion 100 Years After Nobel*, edited by K. K. Kuo, Begell House, New York, 1997, pp. 717–731.